

FORWARD-EULER TIME-DISCRETIZATION FOR WASSERSTEIN GRADIENT FLOWS CAN BE WRONG

YEWEI XU, QIN LI

*Department of Mathematics, University of Wisconsin-Madison, Madison, WI
53706*

ABSTRACT. In this note, we examine the forward-Euler discretization for simulating Wasserstein gradient flows. We provide two counter-examples showcasing the failure of this discretization even for a simple case where the energy functional is defined as the KL divergence against some nicely structured probability densities. A simple explanation of this failure is also discussed.

Keywords. optimal transport, numerical PDEs, numerical methods

1. INTRODUCTION

Minimizing a functional over the space of probability measures is a topic that has garnered tremendous amount of interests over the past few years. The optimization problems emerging from practice are increasingly challenging, and many take the form over the probability measure space:

$$(1) \quad \min_{\rho \in \mathcal{P}(\Omega)} F[\rho]$$

where $\mathcal{P}(\Omega)$ is the collection of all probability measure over the domain $\Omega \subset \mathbb{R}^d$, F is a functional that maps a probability measure to a scalar. Our task is to find, among infinite many possibilities, the probability measure that gives the least value for F . This task can be viewed as an extension from the classical optimization problem usually posed over the Euclidean space \mathbb{R}^d . As a counterpart of the classical gradient descent over \mathbb{R}^d , we now formulate the gradient flow:

$$(WGF) \quad \partial_t \rho = -\nabla_{\mathbf{m}} F[\rho] = \nabla \cdot \left(\rho \nabla \frac{\delta F}{\delta \rho} \right),$$

where \mathbf{m} stands for the chosen metric over \mathcal{P} . If we confine ourselves to \mathcal{P}_2 , the class of probability measures whose second moments are finite, the Wasserstein W_2 metric can be deployed, and the gradient can be expressed explicitly.

The structure of the PDE strongly suggests a particle treatment on the numerical level. Indeed the term $-\nabla \frac{\delta F}{\delta \rho}$ can be simply interpreted as the velocity field. Let X_0 be drawn from ρ_0 , the initial distribution, then driven by this velocity field:

$$(2) \quad \dot{X}_t = -\nabla \frac{\delta F}{\delta \rho} \Big|_{\rho_t} (X_t) \quad \Rightarrow \quad \text{Law}(X_t) = \rho_t \quad \text{for all time.}$$

E-mail address: xu464@wisc.edu, qinli@math.wisc.edu.

Date: June 2024.

In the equation $\nabla \left. \frac{\delta F}{\delta \rho} \right|_{\rho_t}$ means the gradient is evaluated at ρ_t , the solution to (WGF) at time t . Often in practice, this equation cannot be executed since ρ_t is not known ahead of time. So numerically the dynamics is replaced by an ensemble of particles (sometimes also termed the particle method):

$$\rho_t \approx \frac{1}{N} \sum_i \delta_{x_i(t)}, \quad \text{with} \quad \dot{x}_i = -\nabla \left. \frac{\delta F}{\delta \rho} \right|_{\rho_t} (x_i(t)).$$

This is now a coupled ODE system of size Nd . Running ODEs has been a standard practice. Most literature choose an off-the-shelf solver, and the simplest among them is the classical Forward Euler (shorthand by FE throughout the paper). Setting h to be a very small time-stepping, we can march the system forward in time:

$$(3) \quad x_i^{n+1} = x_i^n - h \nabla \left. \frac{\delta F}{\delta \rho} \right|_{\rho^n} (x_i^n),$$

where the superindex stands for the time step, and the lowerindex stands for the choice of the particle. This numerical strategy is vastly popular: Potentially for its simplicity and the lack of counter-argument, it has been the go-to method in many engineering problems, see [1, 24, 27, 25, 13, 19, 9].

We would like to alarm, in our very short note, that this is probably a dangerous practice. In particular, we will give two counter-examples, both framed in the very simple setting where F is a KL divergence against a nicely constructed target distribution, and show that (3) could lead to erroneous answer. In fact, we will go back to a even more fundamental formula (2) and show the forward Euler conducted at this level is problematic.

Both examples use the KL divergence, with the target distribution being very smooth, and log-concave. The specific introduction of the problem has different origins, but they share similar features. FE brings the cascading effect along iteration: It decreases the smoothness of the potential in each iteration, and thus after finite rounds of iteration, the distribution at hand is no longer smooth and no longer has finite Wasserstein derivative. This loss of regularity can be introduced by the non-injectivity of the pushforward map, or can be rooted in the consumption of two derivatives in the update, as will be demonstrated in the two examples respectively.

This discovery might seem surprising at the first glance, but it really resonates the classical discovery in numerical PDEs, where most of solvers perform discretization in space before that in time [16]. This includes the famous ‘‘Method of lines’’ [8] and ‘‘spectral method’’ [10]. At the heart of the thought is usually termed the stability theory: time discretization is restricted by the largest spectrum of the PDE operator at hand. Since PDE operators are typically unbounded, discretization has to be done in space first, to threshold the largest spectrum, allowing finite time-stepping. This thinking is somewhat hidden in particle-method for gradient-flow, but the restriction should not be overlooked.

This discovery also brings us back to the classical proposal in the seminar work of [14], where the authors essentially proposed an implicit Euler solver for advancing (WGF). Largely recognized as non-solvable, efforts have been made towards developing alternatives [20, 22, 17, 18, 12, 4, 6, 15, 26]. Many such alternatives need to go through similar test on stability, but this task is beyond the scope of the current note.

Section 2 collects some classical derivation on Wasserstein derivative. Readers familiar with the matter should feel safe to skip it. Section 3 provides the two counter-examples and the shared general theory that we summarize.

2. BASICS AND NOTATIONS FOR GRADIENT FLOW

We start off with some quick summary of preliminary results.

The problem under study (1) is an optimization over the probability measure space, and it is viewed as an extension of optimization over the Euclidean space, $\min_{x \in \mathbb{R}^d} E(x)$. As a consequence, it is expected that many techniques for $\min_{x \in \mathbb{R}^d} E(x)$ can be carried over. The simplest gradient descent finds x by evolving the following ODE:

$$\dot{x} = \frac{d}{dt}x = -\nabla_x E, \quad \text{so} \quad \lim_{t \rightarrow \infty} E(x(t)) = \min_x E(x),$$

when some properties of E are taken into account, non-asymptotic convergence rate can also be derived.

To translate this strategy to solve problem (1) is not entirely straightforward. The challenge here is two-folded:

- $\mathcal{P}(\Omega)$ is infinite dimensional. In the classical optimization problem, $x \in \mathbb{R}^d$ and is finite-dimensional. $\rho \in \mathcal{P}(\Omega)$ is an infinite dimensional object. To push ρ around necessitates the language of partial differential equation. The PDE will characterize the evolution of $\rho(t, \cdot)$ over $\mathcal{P}(\Omega)$ in time.
- $\mathcal{P}(\Omega)$ is a nonlinear space. Unlike the Euclidean space and the Hilbert function space that can be “normed,” $\mathcal{P}(\Omega)$ is nonlinear, and thus is a manifold. Without a proper definition of the metric, even the term “gradient” is not valid. Due to the nonlinearity, metrics have to be defined locally to measure the distance between two probability measures. Many choices are available [11, 21]. Among them it has been prevalent to deploy the Wasserstein metric [5, 23, 3, 7]. It is a term that is derived from optimal transport theory that measures the length of geodesics between two probability measures. On this metric, one can define the local tangent plane and gradient with respect to this metric. This is the metric that we will use throughout the paper.

Under this metric, it is a standard practice to lift up gradient descent to gradient flow, and we arrive at (WGF).

2.1. Basic Notations. Throughout the paper, we study objects within $\mathcal{P}_2(\mathbb{R}^d)$, the collection of probability measures of finite second moment on \mathbb{R}^d . This space has an important subset $\mathcal{P}_2^r(\mathbb{R}^d)$ that collects all probability measures that are Lebesgue absolutely continuous. Then for any $\rho \in \mathcal{P}_2^r(\mathbb{R}^d)$, we can associate it with a probability density function (pdf) $p : \mathbb{R}^d \rightarrow [0, +\infty)$ such that $d\rho = p dx$. For easier notation, we write $p \propto \exp(-U)$ for some $U : \mathbb{R}^d \rightarrow \mathbb{R}$. We may use ρ and $\exp(-U)$ interchangeably when the context is clear. The measure ρ is said to be log-concave if U is convex, and log-smooth if U is smooth.

Over the space of \mathcal{P}_2 , we define a functional $F : \mathcal{P}_2(\mathbb{R}^d) \rightarrow \mathbb{R}$. For every ρ define the W_2 subgradient of F as:

$$\nabla \left. \frac{\delta F}{\delta \rho} \right|_{\rho},$$

i.e., the gradient of the first variation of F with respect to the measure ρ . We denote $D(|\partial F|)$ the collection of ρ whose subgradient has finite slope in $L_2(\rho)$ ([2, Lemma 10.1.5]), and for $\rho_t \in D(|\partial F|)$, gradient descent continuous-in-time over the Wasserstein metric gives (WGF).

When FE discretization is deployed, we have the updates:

$$(FE) \quad \rho_{k+1} = (\text{Id} - h \nabla \left. \frac{\delta F}{\delta \rho} \right|_{\rho_k})_{\#} \rho_k \quad \text{for } k = 0, 1, 2, \dots$$

with ρ_k standing for the k -th iteration solution, h is the time-stepping step-size. Id is the identity map, and $\#$ is the classical pushforward operator. This is the most standard numerical solver used for (WGF), and has been deployed vastly in literature.

According to the definition of the pushforward operator, for any Borel measure σ on X , $T_{\#}\sigma$ denotes a new probability measure that satisfies:

$$(T_{\#}\sigma)(A) = \sigma(T^{-1}(A)) \quad \text{for any } A \subseteq Y,$$

when the given $T : X \rightarrow Y$. Here T does not have to be invertible, and T^{-1} only refers to the pre-image. As a consequence, if both measures have densities that are denoted by $d(T_{\#}\sigma) = qdy$ and $d\sigma = pdx$, then:

$$(T_{\#}\sigma)(A) = \int_A q(y)dy = \int_{T^{-1}(A)} p(x)dx = \sigma(T^{-1}(A)),$$

When T is a diffeomorphism, by the change of variable formula for measures,

$$(4) \quad q(y) = p(T^{-1}(y)) |J_{T^{-1}}(y)|.$$

where $J_{T^{-1}}$ stands for the Jacobian of the inverse map of T , and $|\cdot|$ means taking the absolute value of the determinant of the given matrix.

2.2. KL Divergence as the energy functional. We pay a special attention to the energy functional that has the form of the Kullback-Leibler(KL) divergence.

Given two probability measures $\mu, \gamma \in \mathcal{P}_2(\mathbb{R}^d)$, the Kullback-Leibler(KL) divergence of μ with respect to γ is defined as:

$$(5) \quad \text{KL}(\mu|\gamma) := \begin{cases} \int_{\mathbb{R}^d} \frac{d\mu}{d\gamma} \ln\left(\frac{d\mu}{d\gamma}\right) d\gamma & \text{if } \mu \ll \gamma, \\ +\infty & \text{Otherwise,} \end{cases}$$

where $\frac{d\mu}{d\gamma}$ is understood in the sense of Radon-Nikodym derivatives. If in addition, μ and γ are absolutely continuous with density functions denoted as e^{-V} and e^{-U} respectively for some differentiable U and V , then

$$F(\mu) := \text{KL}(\mu|\gamma) = \int_{\mathbb{R}^d} (U - V) \exp(-V) dx,$$

and the subgradient (velocity field) is explicitly solvable:

$$(6) \quad \nabla \left. \frac{\delta F}{\delta \mu} \right|_{\mu} (x) = -\nabla V(x) + \nabla U(x).$$

3. COUNTER-EXAMPLES

We provide two counter-examples in subsection 3.1 to invalidate the approach of (FE). The failure of (FE) is rooted in the loss of regularity. According to [2] Section 10, only when $\rho \in D(|\partial F|)$ can we properly define the differential and thus run (WGF) forward in time. We will show that ρ_k will drop out of the set even if ρ_0 is prepared within, putting (WGF) to halt. There are two sources of this error, and the two examples showcase them respectively. One reason for the loss of regularity is the non-injectivity of the pushforward map used to march to ρ_{k+1} from ρ_k . The map sends multiple x 's to the same y , the density accumulates in a certain region, and a jump discontinuity is introduced at the boundary. The second reason for the loss of regularity is the consumption of two derivatives in the pushforward map. As a consequence, every ρ_k has two fewer derivatives than its prior. If ρ_0 has finite regularity, then in finite time, ρ_k drops out of $D(|\partial F|)$, halting the running of (WGF). This argument can be made more precise and we discuss a proposition in subsection 3.2.

These results suggest that even though FE discretization is intuitive, the failure is universal.

3.1. Examples. The two examples shown below respectively point towards two sources of loss of regularity.

Example 1: Loss of regularity due to the noninjectivity of the pushforward map. In the first example, we set

$$F(\rho) = \text{KL}(\rho|e^{-U}), \quad \text{with} \quad U(x) = \frac{x^2}{2} + \frac{x^4}{4} + C_0.$$

This functional is well defined over $\mathcal{P}_2^f(\mathbb{R})$, and the constant C_0 is chosen to normalize the measure:

$$C_0 = \ln \left(\int_{\mathbb{R}} \exp\left(-\frac{x^2}{2} - \frac{x^4}{4}\right) dx \right).$$

We will show the failure of the (FE) approach. Setting the initial condition ρ_0 to be the very simple Gaussian function, by marching forward by just one step of size h , we demonstrate that $\rho_1 \notin D(|\partial F|)$.

Proposition 1. *Assume the initial distribution $\rho_0(x)$ has the density of*

$$p_0(x) = \frac{1}{\sqrt{2\pi}} \exp\left(-\frac{x^2}{2}\right),$$

then for any $h > 0$, the one-time-step solution ρ_1 also has a density p_1 , with p_1 being discontinuous, and thus $\rho_1 \notin D(|\partial F|)$, stopping the application of (FE) to produce ρ_2 .

Proof. According to (FE),

$$\rho_1 = T_{\#} \rho_0 \quad \text{with} \quad T(x) := x - h \left. \nabla \frac{\delta F}{\delta \rho} \right|_{\rho_0} (x).$$

We can explicitly compute p_1 . In particular, calling (6), and noticing

$$V(x) = \frac{x^2}{2} + \ln(2\sqrt{\pi}); \quad U(x) = \frac{x^2}{2} + \frac{x^4}{4} + C_0,$$

we have:

$$(7) \quad T(x) = x - h(\nabla U(x) - \nabla V(x)) = x - hx^3.$$

It is important to notice that T is not one-to-one, as seen in Figure 1.

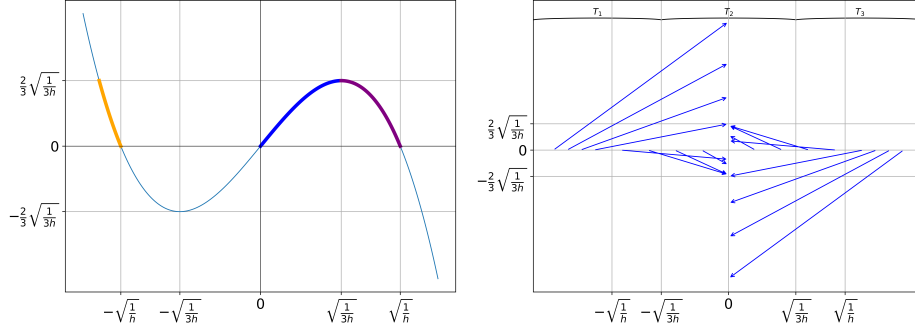


FIGURE 1. The plot on the left shows the pushforward function T . Note that every $y \in (0, \frac{2}{3}\sqrt{\frac{1}{3h}})$ has three pre-image points of x . For example, for $y \in [0, \frac{2}{3}\sqrt{\frac{1}{3h}}]$, the different parts of pre-image are bold-lined: $(-\infty, -\sqrt{\frac{1}{3h}}]$, $[-\sqrt{\frac{1}{3h}}, \sqrt{\frac{1}{3h}}]$ and $[\sqrt{\frac{1}{3h}}, \infty)$ respectively. The plot on the right shows the mapping of T . When T is confined in three parts of the region, denoted as T_1, T_2, T_3 , injectivity is resumed.

In particular, every point in the range of $y \in (0, \frac{2}{3}\sqrt{\frac{1}{3h}})$ has three pre-image points of x . Only confined in smaller x -regions, injectivity is resumed and inversion of T is well-defined, see Table 1. Recall that $T(x) = x - hx^3$, so for any given pair (x, y) such that $T_i(x) = T(x) = y$, we have the determinant of the Jacobian being $|J_{T_i}(x)| = |J_T(x)| = |1 - 3hx^2|$. When $x \neq \pm\sqrt{\frac{1}{3h}}$, we define:

$$|J_i(y)| \doteq |J_{T_i^{-1}(y)}| = \frac{1}{|J_{T_i}(x)|} = \frac{1}{|1 - 3hx^2|}.$$

Map	domain of x	range of y
T_1	$(-\infty, -\sqrt{\frac{1}{3h}})$	$y \in (-\frac{2}{3}\sqrt{\frac{1}{3h}}, +\infty)$
T_2	$(-\sqrt{\frac{1}{3h}}, \sqrt{\frac{1}{3h}})$	$y \in (-\frac{2}{3}\sqrt{\frac{1}{3h}}, \frac{2}{3}\sqrt{\frac{1}{3h}})$
T_3	$(\sqrt{\frac{1}{3h}}, +\infty)$	$y \in (-\infty, \frac{2}{3}\sqrt{\frac{1}{3h}})$

TABLE 1. Range of T in different parts of domains of injectivity.

The loss of such injectivity prevents us to directly apply (4), however, similar derivative nevertheless can be carried out. We focus on $y > 0$ and summarize the calculations here:

- At $y = \frac{2}{3}\sqrt{\frac{1}{3h}}$, there are two points in the pre-image. Since ρ_0 is Lebesgue absolutely continuous, $\rho_1(\{\frac{2}{3}\sqrt{\frac{1}{3h}}\}) = 0$.
- In $(\frac{2}{3}\sqrt{\frac{1}{3h}}, \infty)$, every y has one pre-image point given by T_1^{-1} . Deploying (4), we have:

$$(8) \quad p_1(y) = p_0(T_1^{-1}(y))|J_1(y)|.$$

- In $(0, \frac{2}{3}\sqrt{\frac{1}{3h}})$, every y has three pre-image points given by T_1^{-1} , T_2^{-1} and T_3^{-1} respectively¹. The new density is:

$$(9) \quad p_1(y) = p_0(T_1^{-1}(y))|J_1(y)| + p_0(T_2^{-1}(y))|J_2(y)| + p_0(T_3^{-1}(y))|J_3(y)|.$$

Noting that $\lim_{y \uparrow \frac{2}{3}\sqrt{\frac{1}{3h}}} T_2^{-1}(y) = \sqrt{\frac{1}{3h}} = \lim_{y \uparrow \frac{2}{3}\sqrt{\frac{1}{3h}}} T_3^{-1}(y)$, so

$$(10) \quad \lim_{y \uparrow \frac{2}{3}\sqrt{\frac{1}{3h}}} p_0(T_2^{-1}(y)) = p_0(\sqrt{\frac{1}{3h}}) = \lim_{y \uparrow \frac{2}{3}\sqrt{\frac{1}{3h}}} p_0(T_3^{-1}(y)) > 0,$$

and

$$(11) \quad \lim_{y \uparrow \frac{2}{3}\sqrt{\frac{1}{3h}}} |J_2(y)| = \lim_{x \uparrow \sqrt{\frac{1}{3h}}} \frac{1}{|1 - 3hx^2|} = +\infty = \lim_{x \downarrow \sqrt{\frac{1}{3h}}} \frac{1}{|1 - 3hx^2|} = \lim_{y \uparrow \frac{2}{3}\sqrt{\frac{1}{3h}}} |J_3(y)|.$$

Plugging (10)-(11) back in (9), we notice a blow-up solution at $y = \frac{2}{3}\sqrt{\frac{1}{3h}}$. Comparing (8) and (9), it is now immediate that $p_1(y)$ has a jump discontinuity at $y = \frac{2}{3}\sqrt{\frac{1}{3h}}$, which means the density associated with the probability measure ρ_1 , $\rho_1 \notin W_{\text{loc}}^{1,1}(\mathbb{R})$. By [2, Theorem 10.4.9], $\rho_1 \notin D(|\partial F|)$. The same derivation applies to $p_1(-\infty, -\frac{2}{3}\sqrt{\frac{1}{3h}})$. \square

In this example, the initial condition is a very nice distribution, and the target distribution is log-concave and smooth. Problem is introduced by the non-injectivity of the pushforward map T . More precisely, for $y \in (\frac{2}{3}\sqrt{\frac{1}{3h}}, +\infty)$, only the part T_1 contributes to the density here. For $y = (0, \frac{2}{3}\sqrt{\frac{1}{3h}})$, however, all of T_1, T_2, T_3 contribute to the measure. Since the pushforward densities of T_2 and T_3 are not vanishing at the border of $y = \frac{2}{3}\sqrt{\frac{1}{3h}}$, a jump discontinuity is introduced. Such jump discontinuity is observed for any finite h . As $h \rightarrow 0$, according to (7), $T = x$, also seen in Figure 2. The map converges to the identity map, and the distribution does not move. The problem only occurs to discrete-in-time setting introduced by running (FE).

¹The pushforward measure on $(0, \frac{2}{3}\sqrt{\frac{1}{3h}})$ is equal to $(T_1)_\#(\rho_0|_{T_1^{-1}(\frac{2}{3}\sqrt{\frac{1}{3h}}, -\sqrt{\frac{1}{h}})}) + (T_2)_\#(\rho_0|_{(0, \sqrt{\frac{1}{3h}})}) + (T_3)_\#(\rho_0|_{(\sqrt{\frac{1}{3h}}, \sqrt{\frac{1}{h}})})$, where $\rho_0|_A$ denotes the measure confined on the set A . Each of T_1, T_2, T_3 confined on their domains is a diffeomorphism, and therefore we may apply the change of variable formula to compute the densities of the pushforward measures.

²We should note that it roughly behaves as $\frac{1}{\sqrt[3]{\epsilon}}$ for small ϵ and is an integrable singularity.

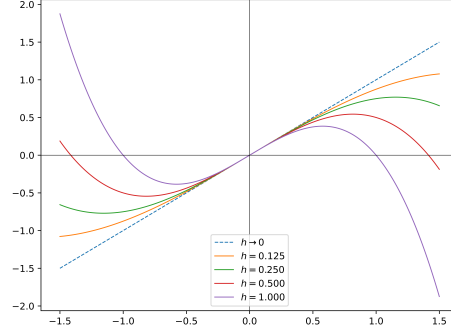


FIGURE 2. Plot of pushforward functions T for different step sizes h . In the $h \rightarrow 0$ limit, $T(x) = x$.

Example 2: Loss of regularity due to the consumption of derivatives. The second example share similar features as the first, but the irregularity is introduced through a different manner. The problem is set as:

$$F(\rho) = \text{KL}(\rho|e^{-U}), \quad \text{with} \quad U(x) = \frac{x^2}{2} + \ln(2\sqrt{\pi}).$$

Here the constant $\ln(2\sqrt{\pi})$ takes care of the normalization. As in the previous example, the energy function is well defined over $\mathcal{P}_2^r(\mathbb{R})$. According to (FE), the pushforward for every iteration is:

$$(12) \quad \rho_{k+1} = (T_k)_\# \rho_k \quad \text{with} \quad T_k(x) := x - h_k \left. \nabla \frac{\delta F}{\delta \rho} \right|_{\rho_k}(x),$$

where $h_k \in (0, 1)$ is the step-size at k -th iteration. We initialize our iteration at ρ_0 with the density

$$(13) \quad p_0(x) = \frac{1}{D_0} \exp(-V_0(x)), \quad \text{with} \quad V_0(x) := \begin{cases} \frac{x^2}{2} & x \in (-1, 1) \\ |x| - \frac{1}{2} & \text{Otherwise} \end{cases},$$

where D_0 stands for the normalization coefficient

$$(14) \quad D_0 = \int_{\mathbb{R}} V_0(x) dx = \sqrt{2\pi} \text{Erf}\left(\frac{1}{\sqrt{2}}\right) + \frac{2}{\sqrt{e}}$$

. The following proposition holds true:

Proposition 2. *Under the conditions stated above:*

- F is 1-convex over $\mathcal{P}_2^r(\mathbb{R})$ with its unique minimizer being $\rho_* = e^{-U}$. The minimum value $F_* = F(\rho_*) = 0$.
- The density function p_1 of ρ_1 , is discontinuous. In addition, $\rho_1 \notin D(|\partial F|)$.
- There are constants $a_k, c_k \in [1, \infty)$ and $b_k \in \mathbb{R}$ so that $p_k(x)$ has the following form:

$$(15) \quad p_k(x) = \begin{cases} \frac{1}{D_0} \exp(-\frac{x^2}{2}) & x \in [0, 1) \\ 0 & x \in [1, c_k) \\ \exp(-a_k x + b_k) & x \in [c_k, +\infty) \\ p_k(-x) & x \in (-\infty, 0) \end{cases}.$$

This proposition immediately evokes our theorem:

Theorem 1. *Under the conditions as in Proposition 2, $F(\rho_k) > 0.019$ for all k .*

Proof. According to the Pinsker's inequality, we have

$$\begin{aligned} F(\rho_k) - F_* &= \text{KL}(\rho_k | e^{-U}) \geq 2 (\text{TV}(\rho_k, e^{-U}))^2 \\ &\geq 2 \left(\int_{-1}^1 (p_k(x) - p(x)) dx \right)^2 \\ &= 2 \left(\left(\frac{1}{\sqrt{2\pi}} - \frac{1}{D_0} \right) \int_{-1}^1 \exp\left(-\frac{x^2}{2}\right) dx \right)^2 \\ &= 4\pi \left(\text{Erf}\left(\frac{1}{\sqrt{2}}\right) \right)^2 \left(\frac{1}{\sqrt{2\pi}} - \frac{1}{\sqrt{2\pi} \text{Erf}\left(\frac{1}{\sqrt{2}}\right) + \frac{2}{\sqrt{e}}} \right)^2 > 0.019. \end{aligned}$$

Here the second inequality comes from lower bounding the total variation using the total variation on the subset $(-1, 1)$; the third line comes from plugging in Equation (13) and Equation (15); the last line comes from using the definition of the normalization constant D_0 in Equation (14); and the last inequality comes from a numerical computation. \square

Proof for Proposition 2. The first bullet point of the proposition is a direct derivation from [2, Theorem 9.4.11]. To show the second bullet point, we compute p_1 explicitly. Following (6), the W_2 -subgradient at ρ_0 is

$$\nabla \frac{\delta F}{\delta \rho} \Big|_{\rho_0} (x) = -\nabla V_0(x) + \nabla U(x) = \begin{cases} x + 1 & x \in (-\infty, -1] \\ 0 & x \in (-1, 1) \\ x - 1 & x \in [1, \infty) \end{cases},$$

meaning the pushforward map is

$$T_0(x) = x - h_0 \nabla \frac{\delta F}{\delta \rho} \Big|_{\rho_0} = \begin{cases} (1 - h_0)x - h_0 & x \in (-\infty, -1] \\ x & x \in (-1, 1) \\ (1 - h_0)x + h_0 & x \in [1, \infty) \end{cases},$$

for step-size h_0 . The inverse and the Jacobian can also be computed explicitly:

$$T_0^{-1}(x) = \begin{cases} \frac{x+h_0}{1-h_0} & x \in (-\infty, -1] \\ x & x \in (-1, 1) \\ \frac{x-h_0}{1-h_0} & x \in [1, \infty) \end{cases}, \quad J_{T_0^{-1}}(x) = \begin{cases} \frac{1}{1-h_0} & x \in (-\infty, -1] \\ 1 & x \in (-1, 1) \\ \frac{1}{1-h_0} & x \in [1, \infty) \end{cases}.$$

Using the change of variable formula for measures, Equation (4) gives

$$\begin{aligned} p_1(x) &= p_0(T_0^{-1}(x)) |J_{T_0^{-1}}(x)| \\ &= \frac{1}{D_0} \begin{cases} \frac{1}{1-h_0} \exp\left(-\frac{x+h_0}{1-h_0} + \frac{1}{2}\right) & x \in (-\infty, -1] \\ \exp\left(-\frac{x^2}{2}\right) & x \in (-1, 1) \\ \frac{1}{1-h_0} \exp\left(-\frac{x-h_0}{1-h_0} + \frac{1}{2}\right) & x \in [1, \infty) \end{cases}. \end{aligned}$$

It is immediate that p_1 has jump discontinuity at $\{-1, 1\}$ two points as long as $h_0 > 0$, and therefore it is not in $W_{\text{loc}}^{1,1}(\mathbb{R})$. Hence $\rho_1 \notin D(|\partial F|)$ according to [2, Theorem 10.4.9].

To prove the third bullet point, we first notice that due to the symmetry, we only need to show the validity of this formula for $x \geq 0$. When $k = 0$, from the

definition in Equation (13), $a_0 = 1, b_0 = \frac{1}{2} - \ln(D_0), c_0 = 1$. Suppose that the claim is true for k , then using (6) and (12):

$$T_k(x) = x - h_k \nabla \frac{\delta F}{\delta \rho} \Big|_{\rho_k} (x) = \begin{cases} x & x \in [0, 1) \\ (1 - h_k)x + a_k h_k & x \in [c_k, \infty) \end{cases}.$$

Noting the monotonicity of T_k allows us to compute the image of T explicitly. In particular:

$$\text{Imag}(T_k|_{[c_k, \infty)}) = [c_{k+1}, \infty), \quad \text{with } c_{k+1} = (1 - h_k)c_k + a_k h_k \geq 1 + (a_k - 1)h_k \geq 1.$$

As a consequence, inverse and Jacobian can be computed:

$$T_k^{-1}(x) = \begin{cases} x & x \in [0, 1) \\ \frac{x - a_k h_k}{1 - h_k} & x \in [c_{k+1}, \infty) \end{cases}, \quad J_{T_k^{-1}}(x) = \begin{cases} 1 & x \in [0, 1) \\ \frac{1}{1 - h_k} & x \in [c_{k+1}, \infty) \end{cases},$$

leading to

$$p_{k+1}(x) = \begin{cases} \frac{1}{D_0} \exp(-\frac{x^2}{2}) & x \in [0, 1) \\ 0 & x \in [1, c_{k+1}) \\ \exp(-a_{k+1}x + b_{k+1}) & x \in [c_{k+1}, +\infty) \\ p_{k+1}(-x) & x \in (-\infty, 0) \end{cases},$$

where a_k and b_k solve:

$$\begin{aligned} \exp(-a_{k+1}x + b_{k+1}) &= p_k(T_k^{-1}(x)) |J_{T_k^{-1}}(x)| \\ &= \frac{1}{1 - h_k} \exp(-a_k \frac{x - a_k h_k}{1 - h_k} + b_k) \\ &= \exp\left(-\frac{a_k}{1 - h_k}x + b_k + \frac{a_k^2 h_k}{1 - h_k} - \ln(1 - h_k)\right), \end{aligned}$$

meaning

$$b_{k+1} = b_k + \frac{a_k^2 h_k}{1 - h_k} - \ln(1 - h_k), \quad a_{k+1} = \frac{a_k}{1 - h_k} > a_k \geq 1.$$

This finishes the proof of induction. \square

3.2. Loss of regularity through (FE) is generic. Both examples showcase the reduced regularity as one propagates ρ_k forward in time according to (FE). This is a generic property that can be shared across FE solver for gradient flow for all functionals of KL divergence type. We extract this property and formulate the following:

Proposition 3. *Let $F(\rho) = \text{KL}(\rho|e^{-U})$ with $U \in \mathcal{C}^\infty(\mathbb{R}^d)$. Assume U is gradient Lipschitz, meaning $\text{Hess}[U] \preceq MI$ for some $M \in (0, +\infty)$. Let $\rho_0 = e^{-V_0}$ for a smooth potential that is $V_0 \in \mathcal{C}^{m+2}(\mathbb{R})$ and $-M_0 I \preceq \text{Hess}[V_0]$ for some $M_0 \in (0, +\infty)$, then the one-step pushforward*

$$\rho_1 = (\text{Id} - h_0 \nabla \frac{\delta F}{\delta \rho} \Big|_{\rho_0})_{\#} \rho_0 = e^{-V_1}$$

has to have reduced regularity. Namely, for $h_0 \in (0, \frac{1}{M+M_0})$, $V_1 \in \mathcal{C}^m$ has two fewer derivatives than V_0 .

Proof. According to the formula (FE) and (12):

$$T_0(x) = x - h_0 \left. \nabla \frac{\delta F}{\delta \rho} \right|_{\rho_0}(x) = x + h_0 \nabla V_0(x) - h_0 \nabla U(x).$$

Since $V_0 \in \mathcal{C}^{m+2}$, $T_0 \in \mathcal{C}^{m+1}$ and its Jacobian is

$$J_{T_0}(x) = I + h_0 \text{Hess}[V_0](x) - h_0 \text{Hess}[U](x) \succ 0.$$

The positivity of the Jacobian comes from the choice of h_0 . It also implies that T_0 is injective, and thus by the Global Inverse Function Theorem, T_0^{-1} is well-defined and $T_0^{-1} \in \mathcal{C}^{m+1}$. Using the change of variable between pushforward measures Equation (4)

$$\begin{aligned} \exp(-V_1(x)) &= \left(\exp(-V_0(T_0^{-1}(x))) \right) \left| J_{T_0^{-1}}(x) \right| \\ &= \exp\left(-\left(V_0(T_0^{-1}(x)) - \ln\left(\left| J_{T_0^{-1}}(x) \right|\right)\right)\right), \end{aligned}$$

namely:

$$V_1(x) = V_0(T_0^{-1}(x)) - \ln\left(\left| J_{T_0^{-1}}(x) \right|\right).$$

Recall that $T_0^{-1} \in \mathcal{C}^{m+1}$ and $V_0 \in \mathcal{C}^{m+2}$, and the Jacobian is taking one higher order of derivative on V_0 , so $\ln\left(\left| J_{T_0^{-1}}(x) \right|\right) \in \mathcal{C}^{m+1}$, and we conclude that $V_1 \in \mathcal{C}^m$. \square

This proposition is generic: as long as (FE) is applied through the form of the gradient flow (WGF), 2 derivatives are lost in every iteration. Any initial data that has finite amount of derivatives will quickly lose hold of their regularity, and falls in the regime where Wasserstein gradient is not even defined. As a consequence, the simple FE stepping should be utilized with caution for gradient flow.

REFERENCES

- [1] D. Alvarez-Melis and N. Fusi. Dataset dynamics via gradient flows in probability space. In M. Meila and T. Zhang, editors, *Proceedings of the 38th International Conference on Machine Learning*, volume 139 of *Proceedings of Machine Learning Research*, pages 219–230. PMLR, 18–24 Jul 2021.
- [2] L. Ambrosio, N. Gigli, and G. Savaré. *Gradient flows in metric spaces and in the space of probability measures*. Lectures in Mathematics. ETH Zürich. Birkhäuser, 2008.
- [3] E. Bernton, P. E. Jacob, M. Gerber, and C. P. Robert. On parameter estimation with the Wasserstein distance. *Information and Inference: A Journal of the IMA*, 8(4):657–676, 10 2019.
- [4] J. A. Carrillo, D. Matthes, and M.-T. Wolfram. Chapter 4 - lagrangian schemes for wasserstein gradient flows. In A. Bonito and R. H. Nochetto, editors, *Geometric Partial Differential Equations - Part II*, volume 22 of *Handbook of Numerical Analysis*, pages 271–311. Elsevier, 2021.
- [5] C. Frogner, C. Zhang, H. Mobahi, M. Araya, and T. A. Poggio. Learning with a wasserstein loss. In C. Cortes, N. Lawrence, D. Lee, M. Sugiyama, and R. Garnett, editors, *Advances in Neural Information Processing Systems*, volume 28. Curran Associates, Inc., 2015.
- [6] G. Fu, S. Osher, and W. Li. High order spatial discretization for variational time implicit schemes: Wasserstein gradient flows and reaction-diffusion systems. *Journal of Computational Physics*, 491:112375, 2023.
- [7] R. Gao and A. Kleywegt. Distributionally robust stochastic optimization with wasserstein distance. *Mathematics of Operations Research*, 48(2):603–655, 2023.
- [8] S. Hamdi, W. E. Schiesser, and G. W. Griffiths. Method of lines. Scholarpedia, 2(7):2859, 2009. Retrieved from <http://www.pdecomp.net/Scholarpedia/MOLfinal.pdf>.
- [9] J. Han, C. T. Ryan, and X. T. Tong. Wasserstein gradient flow for optimal probability measure decomposition, 2024.

- [10] J. S. Hesthaven, S. Gottlieb, and D. Gottlieb. *Spectral Methods for Time-Dependent Problems*. Cambridge Monographs on Applied and Computational Mathematics. Cambridge University Press, 2007.
- [11] S. Ichi Amari. *Information Geometry and Its Applications*, volume 194 of *Applied Mathematical Sciences*. Springer Tokyo, Tokyo, 1 edition, 2016.
- [12] Jacobs, Matt, Lee, Wonjun, and Léger, Flavien. The back-and-forth method for wasserstein gradient flows. *ESAIM: COCV*, 27:28, 2021.
- [13] Y. Jin, S. Liu, H. Wu, X. Ye, and H. Zhou. Parameterized wasserstein gradient flow, 2024.
- [14] R. Jordan, D. Kinderlehrer, and F. Otto. The variational formulation of the fokker–planck equation. *SIAM Journal on Mathematical Analysis*, 29(1):1–17, 1998.
- [15] W. Lee, L. Wang, and W. Li. Deep jko: time-implicit particle methods for general nonlinear gradient flows, 2023.
- [16] R. J. LeVeque. *Finite Difference Methods for Ordinary and Partial Differential Equations*. Society for Industrial and Applied Mathematics, 2007.
- [17] W. Li, J. Lu, and L. Wang. Fisher information regularization schemes for wasserstein gradient flows. *Journal of Computational Physics*, 416:109449, 2020.
- [18] P. Mokrov, A. Korotin, L. Li, A. Genevay, J. M. Solomon, and E. Burnaev. Large-scale wasserstein gradient flows. In M. Ranzato, A. Beygelzimer, Y. Dauphin, P. Liang, and J. W. Vaughan, editors, *Advances in Neural Information Processing Systems*, volume 34, pages 15243–15256. Curran Associates, Inc., 2021.
- [19] S. Neumayer, V. Stein, G. Steidl, and N. Rux. Wasserstein gradient flows for moreau envelopes of f-divergences in reproducing kernel hilbert spaces, 2024.
- [20] G. Peyré. Entropic approximation of wasserstein gradient flows. *SIAM Journal on Imaging Sciences*, 8(4):2323–2351, 2015.
- [21] Y. Polyanskiy and Y. Wu. *Information Theory: From Coding to Learning*. Cambridge University Press, 2024.
- [22] A. Salim, A. Korba, and G. Luise. The wasserstein proximal gradient algorithm. In H. Larochelle, M. Ranzato, R. Hadsell, M. Balcan, and H. Lin, editors, *Advances in Neural Information Processing Systems*, volume 33, pages 12356–12366. Curran Associates, Inc., 2020.
- [23] J. Shen, Y. Qu, W. Zhang, and Y. Yu. Wasserstein distance guided representation learning for domain adaptation. *Proceedings of the AAAI Conference on Artificial Intelligence*, 32(1), Apr. 2018.
- [24] Y. Wang, P. Chen, and W. Li. Projected wasserstein gradient descent for high-dimensional bayesian inference. *SIAM/ASA Journal on Uncertainty Quantification*, 10(4):1513–1532, 2022.
- [25] Y. Yang, S. Eckstein, M. Nutz, and S. Mandt. Estimating the rate-distortion function by wasserstein gradient descent. In A. Oh, T. Naumann, A. Globerson, K. Saenko, M. Hardt, and S. Levine, editors, *Advances in Neural Information Processing Systems*, volume 36, pages 2768–2794. Curran Associates, Inc., 2023.
- [26] R. Yao, L. Huang, and Y. Yang. Minimizing convex functionals over space of probability measures via KL divergence gradient flow. In S. Dasgupta, S. Mandt, and Y. Li, editors, *Proceedings of The 27th International Conference on Artificial Intelligence and Statistics*, volume 238 of *Proceedings of Machine Learning Research*, pages 2530–2538. PMLR, 02–04 May 2024.
- [27] M. Yi, Z. Zhu, and S. Liu. MonoFlow: Rethinking divergence GANs via the perspective of Wasserstein gradient flows. In A. Krause, E. Brunskill, K. Cho, B. Engelhardt, S. Sabato, and J. Scarlett, editors, *Proceedings of the 40th International Conference on Machine Learning*, volume 202 of *Proceedings of Machine Learning Research*, pages 39984–40000. PMLR, 23–29 Jul 2023.